

## Design and improvement of an antipodal Vivaldi antenna

LIU Yu<sup>1</sup>, XIA Xin-Lin<sup>2\*</sup>, YANG Tao<sup>1</sup>

(1. School of Electronic Engineering, University of Electronic Science and Technology of China, Chengdu 611731, China;  
2. Microsystem and Terahertz Research Center, China Academy of Engineering Physics, Chengdu 610200, China)

**Abstract:** In this paper, a novel antipodal Vivaldi antenna (AVA) is presented. The radiation flares were modified by a new composite compound exponential curve. A novel director containing two hybrid elliptical metal patches was adopted to improve the radiation parameters (gain, beam tilts and cross-polarization). The measurement results show that the proposed antenna operates from 1 GHz to more than 40 GHz with peak gain >0 dBi in the range of 1~40 GHz and >12 dBi over the 15~40 GHz range. The squinted beam of E-plane is less than 3° from 3 to 40 GHz and less than 2° from 20 to 40 GHz.

**Key words:** antipodal Vivaldi antenna, wide band antenna, director, millimeter-wave antenna

**PACS:** 84.32.-y, 84.40.Ba

## 一种改进的对拓 Vivaldi 天线设计

刘宇<sup>1</sup>, 夏鑫淋<sup>2\*</sup>, 杨涛<sup>1</sup>

(1. 电子科技大学 电子工程学院, 四川 成都 611731;  
2. 中国工程物理研究院 微系统与太赫兹研究中心, 四川 成都 610200)

**摘要:** 提出了一种新颖的对拓 Vivaldi 天线. 该天线的辐射耀斑用新的复合指数曲线修正. 为改善天线的辐射特性(增益, 波束偏离和交叉极化), 采用了一个新的引向器, 该引向器由两个混合椭圆金属贴片构成. 测试结果表明该天线在 1~40 GHz 频率范围内增益 >0 dBi, 并且在 15~40 GHz 频段内天线的增益 >12 dBi. 在 3~40 GHz 频率范围内, E 面的波束偏离小于 3°, 并且在 15~40 GHz 不超过 2°.

**关键词:** 对拓 Vivaldi 天线; 宽带天线; 引向器; 毫米波天线

中图分类号: TN822+.8, TN952 文献标识码: A

### Introduction

Antennas, especially wideband antenna, play an extreme role in the microwave and millimeter-wave circuits and systems. Various wideband antennas have been proposed in recent years, including stacked patch antenna<sup>[1]</sup>, leaky lens antenna<sup>[2]</sup>, and ridged horn antenna<sup>[3]</sup>. Among the reported designs, the Vivaldi antenna<sup>[4]</sup> is one of the highest potential antennas due to its excellent radiation performances including high gain, simple structure and good directivity.

To broaden the operation bandwidth of Vivaldi antenna, the antipodal Vivaldi antenna, which has two radiant surfaces, was proposed by Gazit. E in 1988<sup>[5]</sup>. This type of antennas has many outstanding performances

such as good directivity, high gain and low cross-polarization level. In the recent reported literatures, various methods have been proposed to improve the radiation characteristics, reduce the size and extend the impedance bandwidth<sup>[6-15]</sup>. In Ref. [6], the author presented a novel approach to improving the impedance matching at low frequencies by Chebyshev tapering. However, the antenna gain is relatively low. In Refs. [7-9], the dielectric lens was adopted to enhance the radiation parameters of Vivaldi antenna. In Ref. [10], the directivity and gain of the proposed AVA has been improved based on introducing a metal patch in the flare aperture. Nevertheless, no obvious improvements were got on the antenna gain at high frequencies (> 25 GHz). In Ref. [11], the SIW technology was used to achieve a Vivaldi antenna with wide operational bandwidth. In addition,

Received date: 2016-06-20, revised date: 2016-12-13

收稿日期: 2016-06-20, 修回日期: 2016-12-13

Foundation items: Supported by the National Natural Science Foundation of China (61271034)

Biography: LIU Yu (1979-), male, Sichuan, China, Ph. D. Research field is RF, microwave, millimeter-wave circuits and systems.

\* Corresponding author; E-mail: xxl0702@sina.cn

the corrugation at the flares was widely used to improve the performance of Vivaldi antenna such as gain<sup>[12-14]</sup>. A reconfigurable wideband Vivaldi antenna was presented in Ref. [15]. Moreover, the ring slot pairs was adopted to generate narrowband multiples.

In this paper, a novel broadband AVA with a new flare shape and a novel director is presented. At first, the inner edges of the radiation flares were defined by a new composite exponential curve. As a result, the antenna gain in high frequencies and low frequencies can be improved by changing different parameters of the composite exponential curve, respectively. In addition, the outer edges of the tapered radiation flares were modified by Chebyshev curve to achieve a wide impedance bandwidth. By using a novel director in front of the antenna's aperture, the beam-tilting in E-plane and antenna gain have been improved significantly. The proposed director containing two parasitic compounded elliptical patches and a half-elliptic substrate can produce strong radiation in the endfire direction. The simulated and measured results show that the antenna can simultaneously obtain a very wide operating bandwidth and excellent radiation characteristics that have both high gain and good directivity.

## 1 Antenna analysis and design

Vivaldi antenna is one of the tapered slot antennas, which has an endfire characteristic. From the radiation mechanism of Vivaldi antenna, the antipodal Vivaldi antenna operates as a resonant antenna at low frequencies and a traveling wave radiator at high frequencies while radiates at different points along the inner edges of the flares. The maximum and lowest operation frequencies are defined by the aperture width (distance between the two opposite flares) at the start of the flares and the mouth of the flares, respectively. In other words, its work band is unlimited in theory. However, different issues occur degrading its radiation performances such as gain reduction, side lobes, beam tilts, and pattern distortion. All of these will severely restrict its applications in high frequencies. The flare shape of the conventional AVA is almost defined by Eq. (1) as follows:

$$x = ae^{(pa \cdot y)} + b, \quad (1)$$

where parameters  $a$  and  $b$  are determined by the dimensions of the antenna. The Vivaldi antenna operates as a resonant antenna at low frequencies. Therefore, to ensure the flare width wide enough ( $\lambda/2$ ) to radiate at 1 GHz, the flare becomes too great. Besides, the gain of AVA is very sensitive to the gradient of the exponential curve. However, Eq. (1) only has one changeable parameter ( $pa$ ). In this case, a new exponential curve should be adopted to overcome this defect.

### 1.1 The modified AVA (MAVA)

As shown in Fig. 1 (a), the modified antipodal Vivaldi antenna (MAVA) mainly consists of two parts. The first section is the tapered balun fed structure modified by a quarter of an ellipse. The second part is the radiation flare constructed by two curves, including the inner and outer edges defined by curves separately.

In this work, the inner edges of the radiation flares are defined by a new composite exponential curve as fol-

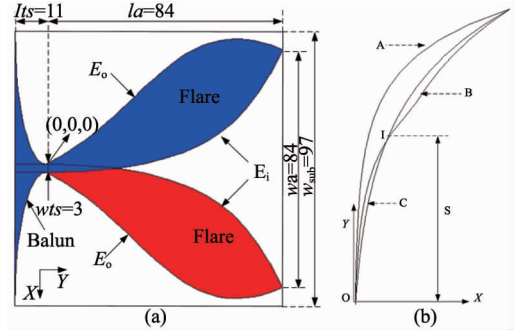


Fig. 1 (a) Structure of the MAVA, (b) the proposed new exponential curve

图1 (a) MAVA 的结构图, (b) 提出的新指数曲线

lows:

$$E_i: x = ae^{f(y)} + b, \quad (2)$$

$$f(y) = pa \cdot y + (pa - pb)(s - y) \left( \frac{\tan^{-1} \left( \frac{y - s}{c} \right)}{\pi} + 0.5 \right), \quad (3)$$

where  $a$  and  $b$  are described by Eq. (4).

$$\begin{cases} a = \frac{wa + wts}{2(m - n)}, m = e^{(pa - pb)(s - la) \left( \frac{\tan^{-1} \left( \frac{la - s}{c} \right)}{\pi} + 0.5 \right)} + pa \cdot la \\ b = -(wts + an), n = e^{(pa - pb) \cdot s \cdot \left( \frac{\tan^{-1} \left( \frac{y - s}{c} \right)}{\pi} + 0.5 \right)} \end{cases}, \quad (4)$$

where  $c$  is a blending coefficient,  $s$  is the value of  $y$  at the intersection point (I),  $la$ ,  $wa$  and  $wts$  are defined in Fig. 1 (a). The new exponential curve (B) shown in Fig. 1 (b) is defined by the combination of curve A and curve C.

In order to reduce some undesired radiation, the sharp edges that cause wave diffraction should be avoided. Moreover, the widened end structure could reduce the size thereby reducing the low operating frequency. As mentioned in Ref. [6], the Chebyshev tapered loading can yield an extremely large impedance bandwidth. Therefore, the outer edges of the radiation flares ( $E_o$ ) were modified by a Chebyshev tapered curve as follows:

$$E_o: x = N((y/lc)^4 - (y/lc)^2), \quad (5)$$

where

$$Lc = \sqrt{(wa/2 - wts)^2 - la^2}, \quad (6)$$

where  $N$  and  $Lc$  were discussed in Ref. [6],  $W_{sub}$ ,  $wts$ ,  $wa$  are defined in Fig. 1 (a).

Figures 2(a) and 2(b) show the results of parametric study on  $s$  and  $pb$  to explain the function of the new composite exponential curve, respectively. By increasing the parameter  $s$ , gain improvement in high frequencies and reduction in low frequency band were observed. Besides, an increase of parameter  $pb$  will result in a gain enhancement in high frequencies ( $> 25$  GHz) and a gain reduction in low frequency band (5 ~ 15 GHz). Therefore, the antenna gain at high frequencies and low frequencies could be improved by changing different parameters of the composite exponential curve, respectively. Even though the proposed MAVA could operate in a very wide frequency band with improved gain characteristic, the antenna gain is relatively low, especially at middle-high frequencies.

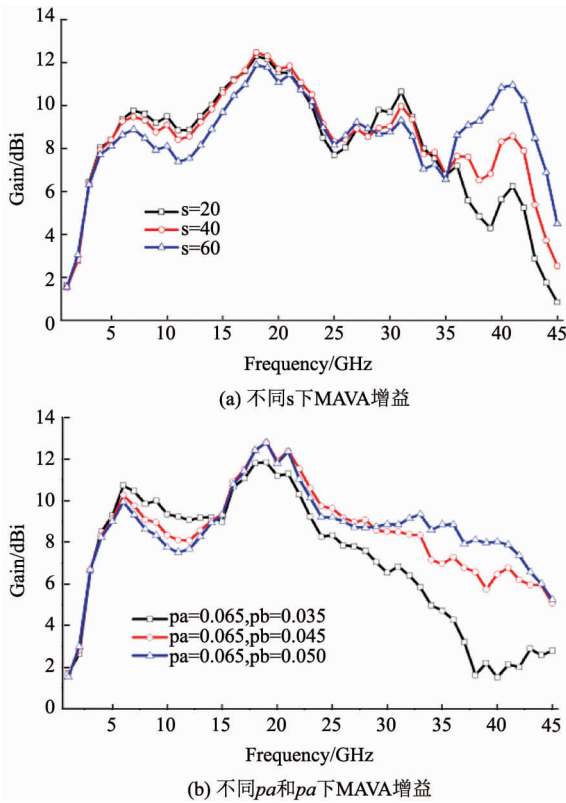


Fig. 2 (a) Gain of MAVA with different  $s$ , (b) gain of MAVA with different  $pa$  and  $pb$   
图2 (a) 不同  $s$  下 MAVA 增益, (b) 不同  $pa$  和  $pb$  下 MAVA 增益

1.2 The modified AVA with a director (MAVA-D)

As shown in Fig. 2, the antenna gain of MAVA degrades severely as the frequency increases. In this work, a metal director was used to improve the radiation characteristic as shown in Fig. 3(a). As discussed in Ref. [10], the metal director located at the antenna aperture is expected to have three different effects. At first, it could direct most of the energy towards the aperture center to improve the beam-tilting over upper working frequencies. Meanwhile, it can broaden the working bandwidth. The last and most important effect is to enhance the field coupling between the flares thereby increasing the antenna gain.

As shown in Fig. 3 (b), the antenna gain for MAVA-D has been improved significantly at middle-high frequencies (Ku-band). The parameter  $de1$  was found to have significant impact on the gain performance with the gain increasing nearly 5 dB as  $de1$  increases from 45 to 75 mm at middle-high frequency ( $> 20$  GHz). However, further increase in  $de1$  causes the gain to decrease. Besides, a bigger increase of parameter  $de1$  will result in a very long antenna extension.

1.3 The modified AVA with a modified director (MAVA-MD)

Even though the gain was enhanced by the metal director, the improvement on the gain is limited to the frequency band up to 25 GHz with relatively low gain. In this work, to further improve the antenna gain in a higher frequency band (Ka-band), a modified director was pro-

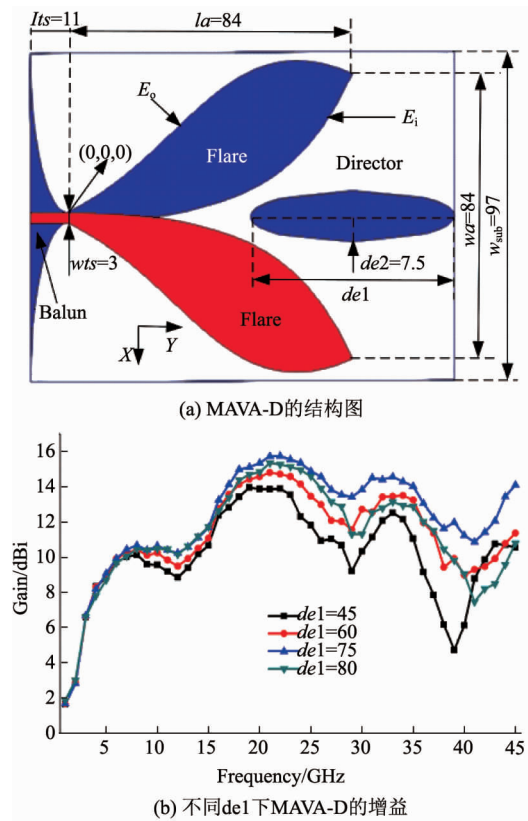


Fig. 3 (a) Structure of the MAVA-D, (b) Gain of MAVA-D with different  $de1$   
图3 (a) MAVA-D 的结构图, (b) 不同  $de1$  下 MAVA-D 的增益

posed as shown in Fig. 5. Compared with the traditional director reported in Ref. [10], this novel director has some distinct advantages. At first, two metal patches located at the top and bottom layers, respectively, were adopted to produce a strong field coupling between the flares. Moreover, the single elliptical metal patch was replaced by a hybrid elliptical patch constructed by a large elliptical patch and a small one. Therefore, the field coupling near the start of the flare, which radiates at high frequencies, could also be enhanced. Finally, the substrate was modified by a half elliptic so that the gain of the antenna could be further improved.

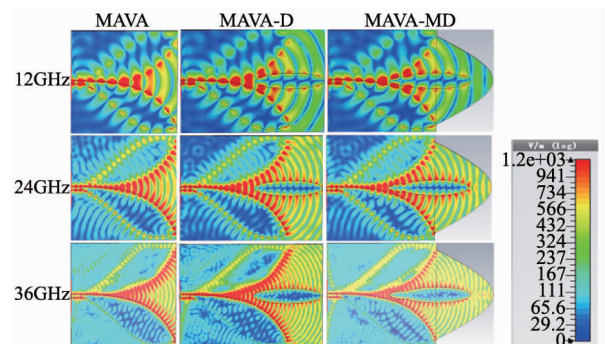


Fig. 4 The electric field distribution for MAVA, MAVA-D and MAVA-MD  
图4 MAVA, MAVA-D 和 MAVA-MD 的电场分布

In order to give a deeper understanding about the effects of the novel director, the electric field distribution for MAVA, MAVA-D and MAVA-MD at 12, 24 and 36 GHz are compared in Fig. 4. It can be seen that strong field coupling to the elliptical metal patch concentrate at the aperture centre with suppression of that at other directions. Clearly, the radiation of MAVA-D is more focused in the endfire direction compared with the MAVA. Besides, the tilted beam can be further compensated in the MAVA-MD.

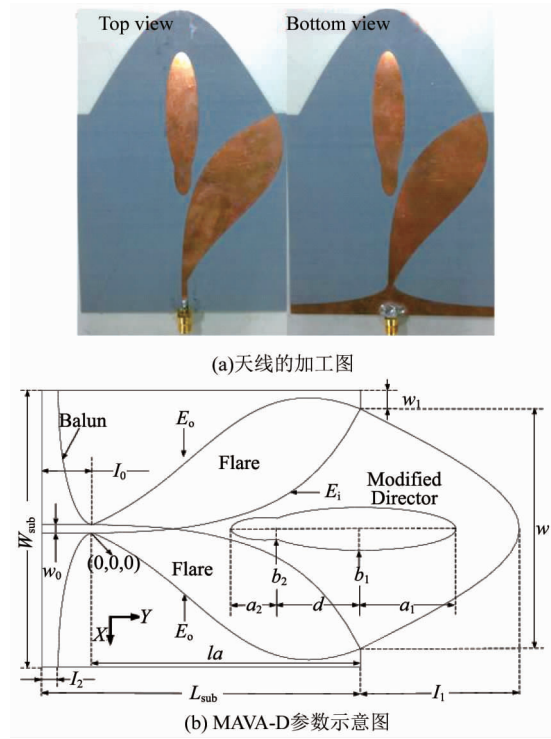


Fig. 5 (a) Photograph of the fabricated antenna, (b) dimensions of the MAVA-MD

图 5 (a) 天线的加工图, (b) MAVA-D 的参数示意图

## 2 Results and discussion

As shown in Fig. 5 (a), a prototype of the proposed

Table 1 Squinting beam and E-plane cross-polarization

表 1 波束偏离和 E 面交叉极化

Frequency/GHz	MAVA		MAVA-D		MAVA-MD	
	Squinting beam/(°)	cross-polarization/dB	Squinting beam/(°)	cross-polarization/dB	Squinting beam/(°)	cross-polarization/dB
4	-16	-16	-6	-23	-3	-28
8	-7	-15	-5	-20	-3	-27
12	-4	-17	-4	-22	-3	-29
16	10	-18	6	-23	3	-28
20	29	-20	5	-30	2	-36
24	26	-14	6	-26	2	-32
28	48	-16	5	-24	1	-33
32	42	-15	4	-25	1	-30
36	38	-13	4	-20	1	-28
40	35	-10	4	-16	1	-24

MAVA-MD was fabricated on Rogers RT5880, which has a relative permittivity 2.2 and the thickness of the substrate is 0.787 mm. The antenna was simulated and optimized using commercial software CST Microwave Studio TM. The final dimensions of the fabricated antenna are (see Fig. 5(b)):  $w_0 = 3$  mm,  $l_0 = 16$  mm,  $w_1 = 6.26$  mm,  $l_1 = 45$  mm,  $a_1 = 30$  mm,  $a_2 = 10$  mm,  $b_1 = 7.5$  mm,  $b_2 = 4$  mm,  $d = 24$  mm,  $l_2 = 5$  mm,  $s = 40$  mm,  $c = 2$ ,  $pa = 0.065$ ,  $pb = 0.05$ ,  $N = 50$ .

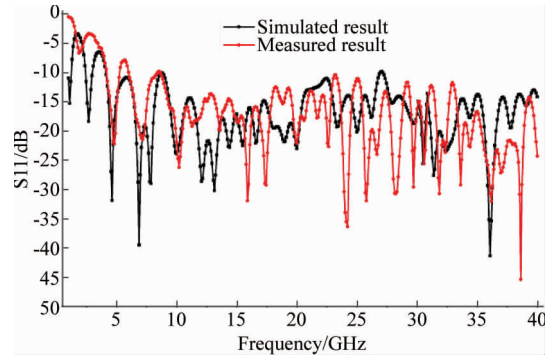


Fig. 6 The measured and simulated S11 of the fabricated MAVA-MD

图 6 加工的 MAVA-MD 的测试和仿真 S11

The S11 was measured with Agilent Network Analyzer N5225A. As can be seen from the Fig. 6, the return loss is less than 10 dB from 4 GHz to 40 GHz. The discrepancies between simulation and measurement may be due to unexpected fabrication and assembly errors. In addition, the connection loss between the printed circuit board and SMA connector, and the unstable substrate parameters may also deteriorate S11, which is not included in the simulations.

Within the frequency range of 4 to 40 GHz, a quantitative comparison of the beam-tilting and cross-polarization in boresight direction of E-plane are contained in Table 1. For MAVA, the squinted beam of E-plane  $> 10^\circ$  at middle-high frequencies ( $> 20$  GHz) and  $> 22^\circ$  from 32 to 40 GHz, while the MAVA-D has a maximum of  $6^\circ$  beam squinting in these frequencies. Moreover, the proposed MAVA-MD can further improve the beam tilting, which shows that it has better resistance on beam

tilting at upper frequency band than MAVA and MAVA-D. Furthermore, the proposed MAVA-MD has a better cross-polarization compared with the MAVA and MAVA-D.

The measured and simulated E-plane and H-plane radiation patterns at 4, 6, 10, 15, 20, 25, 30, 35 GHz are shown in Figs. 7-8, respectively. Due to the proposed modified director acting as a guiding structure, the proposed antenna has symmetric radiation patterns and good endfire characteristic with the main lobe directing in the axial direction (Y-direction in Fig. 5 (b)).

The measured and simulated gain of the proposed antenna is shown in Fig. 9. Obviously, the gain of the MAVA-MD has been improved greatly. The peak gain of

MAVA-MD  $> 12$  dBi for frequencies more than 15 GHz and  $> 14$  dBi over the frequency range of 15 to 40 GHz. Compared with the MAVA, the modified antipodal Vivaldi antenna with a director (MAVA-D) has a better gain characteristic with the gain change increasing nearly 5.5 dB in middle-high frequencies ( $> 20$  GHz). Besides, the antenna gain has been further increased about 6dB owing to the modified director.

As shown in Fig. 10, the proposed MAVA-MD has more firm resistance on beam tilts compared with MAVA. In addition, the MAVA-MD has lower back-lobe and side lobe in comparison with MAVA and MAVA-D.

Table 2 lists out the comparison in terms of size, operation bandwidth, relative permittivity, and gain be-

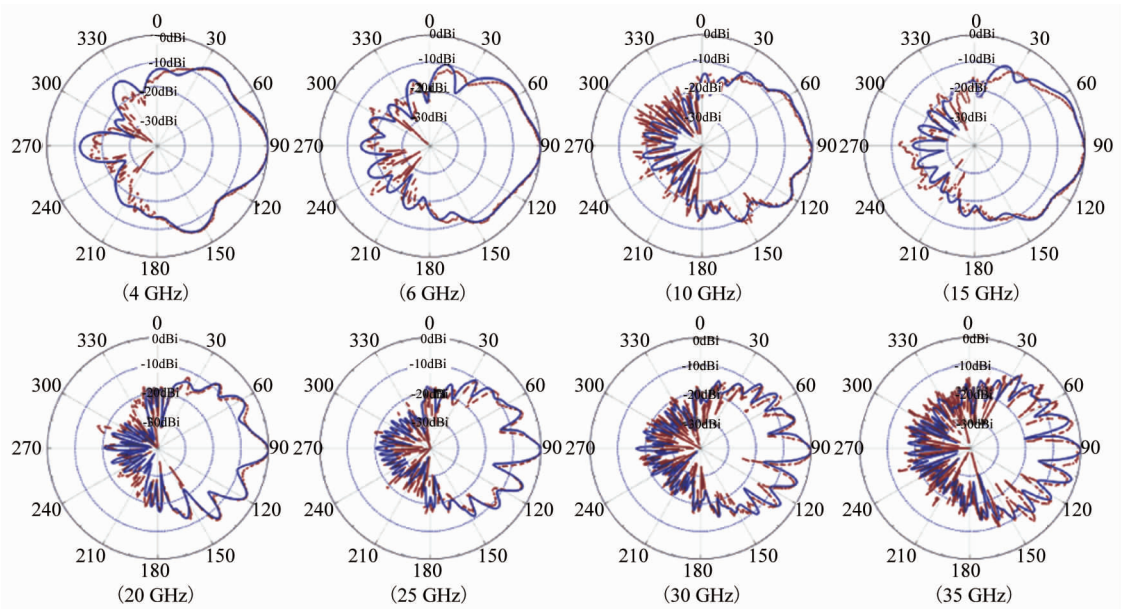


Fig. 7 The measured (solid line) and simulated (dashed line) radiation patterns of E-plane  
图7 E面的测试(实线)和仿真(虚线)方向图

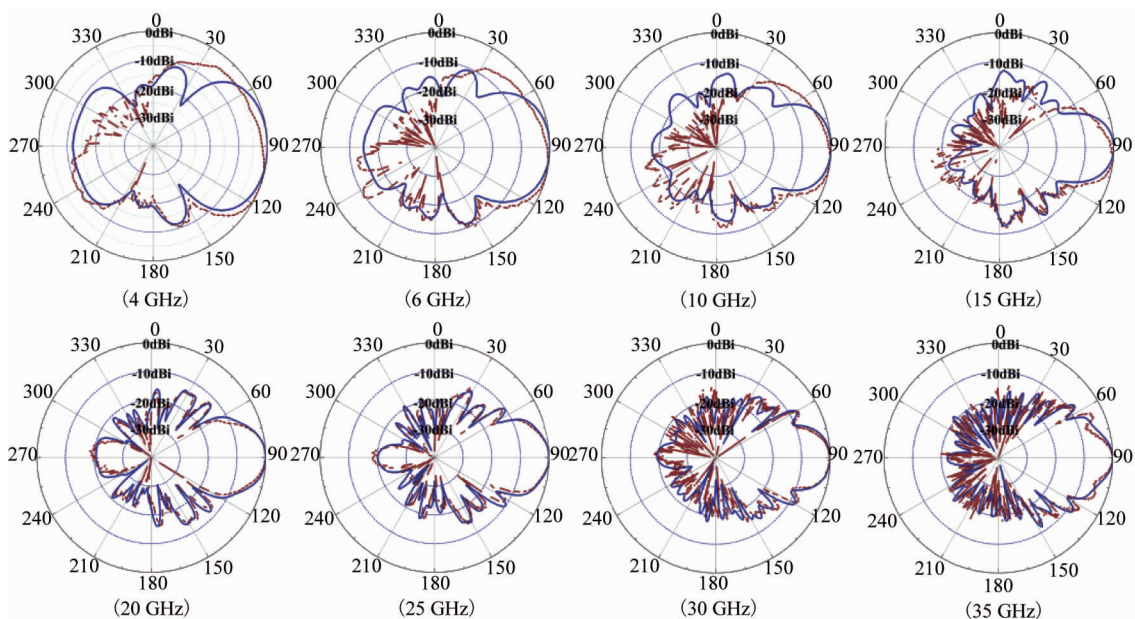


Fig. 8 The measured (solid line) and simulated (dashed line) radiation patterns of H-plane  
图8 H面的测试(实线)和仿真(虚线)方向图

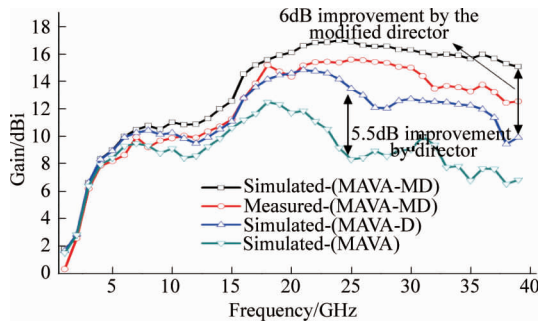


Fig. 9 The gain for the MAVA, MAVA-D and MAVA-MD  
图9 MAVA,MAVA-D 和 MAVA-MD 的增益对比

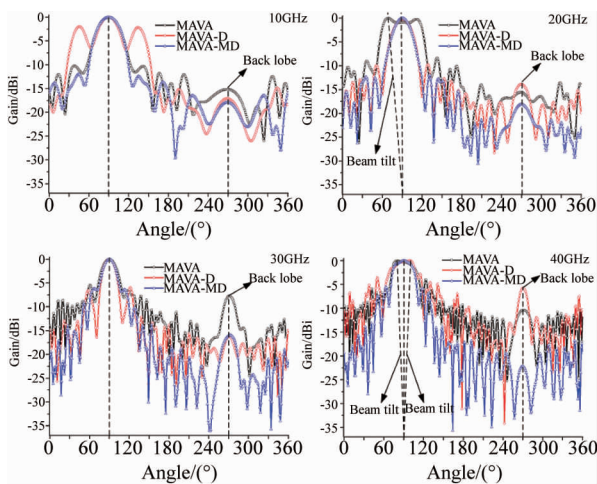


Fig. 10 The simulated radiation patterns of H-plane for the MAVA, MAVA-D and MAVA-MD  
图10 MAVA,MAVA-D 和 MAVA-MD 的 H 面仿真辐射方向图

tween the proposed antenna and antennas from literatures. Clearly, the proposed antenna has some distinct advantages such as a very wide operation bandwidth and a high gain with similar size.

**Table 2 Comparison of the proposed antenna with literatures**  
**表2 文中天线与其他文献中的性能对比**

Ref.	Dimensions/mm <sup>3</sup>	Relative permittivity	O. B. W. /GHz	Freq./GHz→Gain/dBi
[6]	97 × 95 × 1.6	4.4	1 – 35	10→6.2, 20→5.8, 35→4.3
[7]	100 × 140 × 0.8	3.38	2 – 18	10→9, 18→12.2
[8]	70 × 140 × 3	2.2	1.5 – 15	10→11.2, 15→13.5
[9]	50 × 166 × 3.15	2.55	3.0 – 18	3.5→2, 18→12
[10]	66 × 140 × 1.5	2.94	2.0 – 32	10→11, 20→10.2, 30→5
[11]	120 × 160 × 1.6	3.45	2 – 18	N. M
[12]	52 × 145 × 0.508	2.2	3.1 – 10.6	5→9.4, 11→12
[13]	190 × 42 × 0.8	3.3	2 – 18	2→1, 18→13
[14]	78.76 × 91 × 0.508	3.38	3 – 16	3→5.2, 16→10.5
[15]	92 × 106 × 1.6	4.7	1.5 – 5	N. M
This work (MAVA-MD)	96.52 × 140 × 0.787	2.2	1 – 40	10→10.7, 25→15.6, 40→12.7

'O. B. W.' states the operating bandwidth; 'N. M' represents "not mentioned"

### 3 Conclusion

In this paper, a novel antipodal Vivaldi antenna is

presented with good radiation characteristics operating from 1 GHz to over 40 GHz (SMA connector and measurement limit). A new radiation flare shape combining two exponential curves was used to improve the gain characteristic. Moreover, the radiation flares were modified by a Chebyshev curve to achieve an extremely large impedance bandwidth. The antenna gain has been significantly enhanced by adopting a novel director. The proposed antenna exhibits satisfactory radiation characteristics such as low cross-polarization level, high gain of 12 ~ 15 dBi (10 ~ 40 GHz), stable radiation patterns and a wide operation bandwidth that make this antenna suitable for applications in phased array, microwave and millimeter-wave systems, and target RCS imaging, etc.

### References

- [1] Nilavalan R, Craddock I J, Preece A, *et al.* Wideband microstrip patch antenna design for breast cancer tumour detection [J]. *IET Microwaves, Antennas & Propagation*, 2007, **1**(2):277 – 281.
- [2] Bruni S, Neto A, Marliani F. The ultrawideband leaky lens antenna [J]. *IEEE Transactions on Antennas and Propagation*, 2007, **55**(10):2642 – 2653.
- [3] Morgan M A, Boyd T A. A 10-100-GHz double-ridged horn antenna and coax launcher [J]. *IEEE Transactions on Antennas and Propagation*, 2015, **63**(8): 3417 – 3422.
- [4] Gibson P J. The Vivaldi aerial [C]. 1979 European Microwave Conference, Proc.9th, 1979: 101 – 105.
- [5] Gazit E. Improved design of the Vivaldi antenna [J]. *Microwaves, Antennas and Propagation, IEE Proceedings H*, 1988, **135**(2):1091 – 1096.
- [6] Gorai A, Karmakar A, Pal M, *et al.* A super wideband Chebyshev tapered antipodal Vivaldi antenna [J]. *International Journal of Electronics and Communications (AE?)*, 2015, **69**(9): 1328 – 1333.
- [7] Arezoomand, Afsaneh S, Sadeghzadeh R A, *et al.* Investigation and improvement of the phase-center characteristics of VIVALDI's antenna for UWB applications [J]. *Microwave and Optical Technology Letters*, 2016, **58**(6):1275 – 1281.
- [8] Lei J, Fu G, Yang L, *et al.* A modified balanced antipodal Vivaldi antenna with improved radiation characteristics [J]. *Microwave and Optical Technology Letters*, 2013, **55**(6):1321 – 1325.
- [9] Molaei A, Kaboli M, Mirtaeheri S A, *et al.* Dielectric lens balanced antipodal Vivaldi antenna with low cross-polarisation for ultra-wideband applications [J]. *IET Microwaves, Antennas & Propagation*, 2014, **8**(14):1137 – 1142.
- [10] Nassar I T, Weller T M. A Novel Method for Improving Antipodal Vivaldi Antenna Performance [J]. *IEEE Transactions on Antennas and Propagation*, 2015, **63**:3321 – 3324.
- [11] Zarrabi F B, Gandji N P, Ahmadian, R, *et al.* Modification of Vivaldi Antenna for 2 – 18 GHz UWB Application with Substrate Integration Waveguide Structure and Comb Slots [J]. *Applied Computation Electromagnetics Society Journal*, 2015, **30**(8): 844 – 849.
- [12] In D M, Lee M J, Kim, D, *et al.* Antipodal linearly tapered slot antenna using unequal half-circular defected sides for gain improvements [J]. *Microwave and Optical Technology Letters*, 2012, **54**(8):1963 – 1965.
- [13] Sato H, Takagi Y, Sawaya K. High Gain Antipodal Fermi Antenna with Low Cross Polarization [J]. *IEICE Transactions on Communications*, 2011, **E94B**(8): 2292 – 2297.
- [14] Huang T J, Chiang C Y, Hsu H T. Effect of Corrugation Profiles on the Improvement of Front-to-back Ratio for Dual Exponentially Tapered Slot Antennas (DETSAs) [C]. 2011 Proceedings of the Asia-Pacific Microwave Conference.
- [15] Yim T L, Rahim S K A, Dewan R. Reconfigurable wideband and narrowband tapered slot Vivaldi antenna with ring slot pairs [J]. *Journal of Electromagnetic Waves and Applications*, 2013, **27**(3): 276 – 287.